A Hierarchical Approach to Quantum Many-Body Systems in Structured Environments

Kai Müller,[1] Kimmo Luoma,[2] and Christian Schäfer[3, 4, *]

[1]*Institut für Theoretische Physik, Technische Universität Dresden, D-01062 Dresden, Germany.*
[2]*Department of Physics and Astronomy, University of Turku, 20014 Turku, Finland.*
[3]*Department of Physics, Chalmers University of Technology, 412 96 Göteborg, Sweden*
[4]*Department of Microtechnology and Nanoscience, MC2,*
Chalmers University of Technology, 412 96 Göteborg, Sweden
(Dated: May 9, 2024)

Cavity quantum materials combine the rich many-body physics of condensed matter systems with strong coupling to the surrounding electromagnetic field, which presents both novel prospects and intricate challenges. One is often interested in the properties of one specific aspect of the material, e.g. the electronic many-body dynamics, subject to a structured bath of phononic and photonic modes. Open quantum systems featuring non-Markovian dynamics are routinely solved using techniques such as the Hierarchical Equations of Motion (HEOM) but their usage of the system density-matrix renders them intractable for many-body systems. Here, we combine the HEOM with the Bogoliubov–Born–Green–Kirkwood–Yvon (BBGKY) hierarchy to reach a consistent and rigorous description of open many-body systems and their quantum dynamics. We demonstrate first the strength and limitations of this stacked hierarchy for superradiant emission and spin-squeezing of established quantum optical models before presenting its full potential for quantum many-body systems. In particular, we explicitly simulate the impact of charge noise on the dynamic of the Fermi-Hubbard model subject to a structured bath comprising cavity and vibro-phononic environment. Strong optical coupling not only modifies the dynamic of the many-body system but serves furthermore as measurement channel providing information about the correlated motion imprinted by charge noise. Our work establishes an accessible, yet rigorous, route between condensed matter and quantum optics, fostering the growth of a new domain at their interface.

Please note, this early version will be refined and updated with additional results in the near future.

I. INTRODUCTION

The ability to control many-body quantum systems with quantized light is imperative in modern quantum technologies such as photonics, quantum memories, quantum sensing, or quantum information.[1–4] An idealized description of the fundamental building block, the quantum emitter, is challenged by disturbances, such as charge noise or phonon scattering, that hint at the inherent many-body character of each quantum system. Strong light-matter coupling allows to control interactions over extended length scales[5–9], holding promise to design materials [10–12], devices [13, 14], or even chemical properties [15–19] non-intrinsically and on demand. The many-body physics originating from electronic and vibrational structure, as well as their respective decoherence, is crucial for a comprehensive understanding and refinement of this control-strategy.[20–24]

Our primary challenge in this study is to address physical processes wherein many-body interactions, strong light-matter coupling, and strong system-environment coupling are all fundamental. Achieving this goal necessitates combining concepts from quantum optics and solid-state physics. Quantum optics often treats light-matter interaction non-perturbatively but simplifies the structure of materials drastically. Conversely, condensed matter or quantum chemistry approaches accurately describe the material system but oversimplify interactions with surrounding environments. Our aim is to bridge quantum optical and condensed matter/quantum chemistry approaches to create a framework for studying the effects of strong light-matter coupling on many-body physics more efficiently than previously possible.

One approach to handle non-Markovian dynamics is to resort exact numerical methods, where the effects of the environment are taken into account stochastically. These methods could be wave function based, such as non-Markovian Quantum State Diffusion (NMQSD) [25–27] or density matrix based such as the Hierarchical Equations Of Motion (HEOM) [28, 29]. In this work we focus on the latter approach. HEOM has been used to solve a large variety of problems such as the dynamics of the Holstein polaron [30] or the problem of coupling to multiple environments [31]. To use HEOM, the bath correlation function, which measures the response of the environment to the open system needs to be fitted with exponential functions [32]. The resulting hierarchy couples the physical density matrix to auxiliary density matrices, and the hierarchy's depth depends on the system-environment coupling strength. However, this approach becomes impractical for many-body systems due to the exponential scaling of physical and auxiliary states with system size. Our aim is to combine the HEOM approach

* Electronic address: christian.schaefer.physics@gmail.com

with an efficient strategy for many-body dynamics.

The second challenge to face is the strong coupling between the material system and the cavity field. Micro- and plasmonic cavities will often require the consideration of multiple modes [13, 33]. Commonly used approaches, such as adiabatic elimination [34] or mean field [35], show at best limited success at approximating the exact dynamic. Cluster expansion techniques for the light matter interaction [36, 37] and HEOM related expansions for the material system alone have been proposed [38, 39] but they still suffer from poor scaling for many-body quantum systems. Entering the ultrastrong coupling regime [40], counter-rotating [41] and self-polarization terms [42, 43] become essential which necessitates the usage of the correct Lindblad dissipator that connect between the correlated eigenstates. In this work, we will limit ourselves to the strong coupling regime where such effects play a subordinate role.

Lastly, the third challenge is to control the exponential scaling of the many body system. Wavefunction-based approaches, such as tensor networks [44] or matrix product states, increase exponentially in cost over time which limits their use to short time-scales [45, 46]. Non-equilibrium Green functions approaches made recent progress after the successful integration of the generalized Kadanoff-Baym ansatz [47, 48] but a consistent treatment of complex structured baths remains challenging. An attractive approach with good scaling properties is to perform a cluster expansion of the density matrix into single-,two-,three- and N-body reduced density matrices and then truncate the resulting Bogoliubov–Born–Green–Kirkwood–Yvo (BBGKY) hierarchy at some low order [49, 50].

Here, we combine BBGKY and HEOM to establish a stacked BBGKY-HEOM hierarchy that provides an efficient framework for the simulation of correlated manybody systems subject to structured baths. The remainder of this article is structured as follows: Sec. II provides a short introduction to non-Markovian open-system and many-body theory before the derivation of the BBGKY-HEOM equations in Sec. II B. We illustrate their performance, limitation, and associated physical intuition for various systems in Sec. II. In particular, Sec. III A demonstrates that BBGKY-HEOM succeeds in reproducing the quantum many-emitter physics in the superradiant driven Tavis-Cummings model while retaining constant scaling with emitter size. We subsequently shift our focus to many-body electronic systems in the form of the Fermi-Hubbard model coupled to a lossy cavity mode and subject to charge noise in Sec. III B. This system in then embedded into a highly structured bath in Sec. III C that represents phononic motion in organic crystals. The BBGKY-HEOM provides accurate predictions for as long as the onsite repulsion U, and with it the degree of electronic correlation, remains moderate. We notice that the bath adds a stabilizing contribution to the BBGKY equations. Sec. IV finally concludes our study and provides an outlook into the nearer future.

II. THEORY

A material comprising electrons and nuclei moving at non-relativistic velocities is described by Schrödinger's equation. Its interplay with electromagnetic fields necessitates the consideration of the (quantized) normal modes of the Maxwell equations. This combined system can be described using the minimal coupling Hamiltonian. In Coulomb gauge,

$$
\hat{H} = \sum_{i=1}^{N_e+N_n} \frac{1}{2m_i} \left[-i\hbar \boldsymbol{\nabla}_i - q_i \hat{\mathbf{A}}(\mathbf{r}_i) \right]^2 + \hat{H}_{\parallel} \\
+ \frac{\varepsilon_0}{2} \int dr^3 \left[\hat{\mathbf{E}}_{\perp}(\mathbf{r})^2 + \hat{\mathbf{B}}(\mathbf{r})^2 \right]
\tag{1}
$$

for N_e electrons and N_n nuclei with charge q_i and mass m_i. We will use atomic units in the following. Eq. (1) treats the transversal degrees separate from the longitudinal and instantaneous Coulombic interactions $H_{\parallel}$. The latter includes electronic and nuclear interactions which are typically treated in first quantization at first

$$
\hat{H}_{\parallel} = \hat{V}_{ee} + \hat{V}_{en} + \hat{V}_{nn}; \quad \hat{V}_{ee} = \sum_{\substack{i \neq j}}^{N_e} \frac{1}{|\mathbf{r}_i - \mathbf{r}_j|} \\
\hat{V}_{en} = \sum_{i,j}^{N_e,N_n} \frac{-q_i}{|\mathbf{r}_i - \mathbf{R}_j|}; \quad \hat{V}_{nn} = \sum_{\substack{i \neq j}}^{N_n} \frac{q_i q_j}{|\mathbf{R}_i - \mathbf{R}_j|}.
\tag{2}
$$

Their interplay results in rich many-body physics that gives rise to electronic, vibronic, and phononic structure and, unfortunately, to an exponentially increasing complexity. The system-bath strategy aims now at identifying the smallest possible subsystem that we can treat explicitly while absorbing the remainder into a bath[51]. First step is to simplify the Hamiltonian to a form that contains only linear interactions between various subsystems

$$
\hat{H}_{tot} = \hat{H}_{sys} + \hat{H}_B + \hat{H}_{sys,B}.
\tag{3}
$$

Such a separation can be formalized using the projection operators P and $Q = 1 - P$, which are defined in such a way that the relevant state of the subsystem is obtained by projecting the total state $\rho_{tot}(t)$ to the relevant subspace

$$
\rho_{sys}(t) = P\rho_{tot}(t).
\tag{4}
$$

A common choice is $P\rho_{tot}(t) = \text{Tr}_{sys}\{\rho_{tot}(t)\} \otimes \rho_B$, where ρ_B is some fixed reference state. Typically it is also assumed that at some specific initial time t_0, the total state is a product $\rho(t_0) = \rho_{sys}(t_0) \otimes \rho_B$. Moreover, it is often possible to choose the partitioning of the Hamiltonian in such way that the odd moments of the interaction term vanish with respect to the reference state (a typical situation is for example the case where ρ_B corresponds to the thermal state of a quadratic bosonic bath to which the open system couples linearly).

The gauge freedom of the electromagnetic modes provides various different paths. An intuitive approach is to isolate the bilinear term $\sum_i -i\hbar q_i/m_i \hat{\mathbf{A}}(\mathbf{r}_i) \cdot \boldsymbol{\nabla}_i$ as coupling operator and absorb the quadratic diamagnetic term into dressed photonic operators[42, 43]. A second direction, often more promising for finite systems, is to shift into the multi-polar gauge (detailed in App. C). Combination with the long-wavelength approximation provides then a simple bilinear coupling between dipole moment and displacement field. In addition, self-polarization terms modify the dynamic of the system and the redefinition of the optical creation and annihilation operators introduce the need to reconsider the interpretation of system and bath. Vibrational and phononic interaction follow similarly. The influence of nuclei motion on the electron-nuclear interaction can be expanded around the equilibrium configuration

$$\hat{V}_{en} \approx \hat{V}_{en}|_0 + \sum_j \delta\mathbf{R}_j \cdot \boldsymbol{\nabla}_j \hat{V}_{en}|_0 + ... \qquad (5)$$

and truncated at harmonic order, resulting in a bilinearly coupled electron-phonon or electron-vibration coupling that depends on the electronic configuration. Note that also here second-order (known as Debye-Waller) corrections appear that require to carefully scrutinize the separation between system and bath.[52] The following derivations and demonstrations are agnostic to such subtleties as we will focus on the development and illustration of the BBGKY-HEOM methodology. A thorough derivation of system-bath couplings for a specific physical realization is evidently essential for meaningful predictions but it is not the focus of this manuscript.

A. Many-body Open Quantum Systems beyond the Markovian Limit

Very often the environment can be modeled as a collection of non-interacting quantum harmonic oscillators. This is for example frequently the case in quantum optics [53], or when the system is coupled weakly to a large number of degrees of freedom where central limit type of arguments yield an approximately Gaussian response [54]. When a description of the environment in terms of harmonic oscillators is suitable, then the HEOM approach yields an exact description for the evolution of the open quantum system [28, 29, 55]. In fact, HEOM type of techniques can be even extended to cases where the environment is anharmonic [56, 57]. In this work, we focus on the case of harmonic baths, either corresponding to optical modes confined in an imperfect cavity or a phonon bath into which a quantum emitter is embedded. The influence functional of the bath can then be computed exactly under the harmonic assumption when using the path integral formalism [58]. HEOM follows from this influence functional [29] and we provide a sketch of the derivation for the open system in App. D.

Following the previous motivation, we start with a many-body system that is linearly coupled to a collection of harmonic oscillators. Especially in the case of cavity quantum materials many different environments (e.g. phonon- and electromagnetic environment) can be relevant for the problem. We label these distinct environments with k, such that the bosonic annihilation (creation) operators belonging to mode λ of bath k are given by a_λ^k ($a_\lambda^{k\dagger}$). The evolution of the total state ρ_{tot} of system and environments is then described by

$$\dot{\rho}_{tot} = -i[H, \rho_{tot}], \qquad (6)$$
$$H = H_{sys} + \sum_{k,\lambda} g_\lambda^k (L^k a_\lambda^{k,\dagger} + L^{k\dagger} a_\lambda^k) + \sum_\lambda \omega_\lambda^k a_\lambda^{k\dagger} a_\lambda^k, \qquad (7)$$

where L^k is the system operator that describes the coupling to environment k and ω_λ^k, g_λ^k are the frequencies and coupling strengths of the respective modes. The environments are characterized by their spectral density $J_k(\omega) = \sum_\lambda |g_\lambda^k|^2 \delta(\omega - \omega_\lambda^k)$ or equivalently by their bath correlation function $\alpha_k(\tau) = \int_0^\infty J_k(\omega) e^{-i\omega\tau} \mathrm{d}\tau$. We are foremost interested in the reduced dynamics in the system Hilbertspace $\mathcal{H}_{sys}$ but it should be noticed that HEOM keeps track of the bath degrees of freedom. For the moment, the N particles of the many-body Hamiltonian are assumed to behave identical under a single particle Hamiltonian H_i and experience two-particle interactions V_{ij}. In addition, we assume identical coupling to the environments via the single particle operator L_i^k, such that the many-body Hamiltonian and the coupling operators can be decomposed into

$$H_{sys} = \sum_{i=1}^N H_i + \sum_{i \neq j}^N V_{ij}, \quad L^k = \sum_{i=1}^N L_i^k. \qquad (8)$$

The evolution equation (6) is therefore invariant under particle exchange. Such assumptions are natural for indistinguishable particles but one can easily relax this condition if one would like to describe for example ensembles of inhomogeneously broadened emitters.

B. Combining HEOM with BBGKY

Despite the restrictions employed above, the resulting system-bath Hamiltonian applies to a vast range of systems, from typical quantum optical setups over Rydberg ensembles to molecules in cavities. However, due to the large size of the Hilbert space it is typically not possible to diagonalize Eq. (6) exactly.

Starting point for the derivation of a holistic description that combines many-body and system-bath dynamic is the HEOM equation. We present in the following only the equations for a single environment for the sake of simplicity but note that the extension to multiple environments is trivial and will be illustrated in Sec. III C.

The HEOM equation accounts for the non-Markovianity of the coupled environment with an infinite set of coupled equations for the system density matrices $\rho_{sys}^{(n,m)} \in \mathcal{H}_{sys}$. Here, $\rho_{sys}^{(0,0)} = \mathrm{Tr}_B(\rho_{tot}) =: \rho$ is the reduced density matrix of interest and m, n are vector indices labelling (unphysical) auxiliary density matrices. The hierarchy is truncated at a sufficiently high order which is determined by the non-Markovianity of the system-bath interaction, i.e., a Markovian bath corresponds to a truncation at first order according to $\rho_{sys}^{(e_k,0)} \propto L\rho_{sys}^{(0,0)}$, $\rho_{sys}^{(0,e_k)} \propto \rho_{sys}^{(0,0)} L^\dagger$. The evolution equation for the auxiliary density matrices (including the physical reduced density matrix $\rho_{sys}^{(0,0)}$) reads

$$
\begin{aligned}
\dot{\rho}_{sys}^{(n,m)} =\ & -i[H_{sys}, \rho_{sys}^{(n,m)}] - (w \cdot n + w^* \cdot m)\, \rho_{sys}^{(n,m)} \\
& + \sum_{k=1}^{M} \Bigg(G_k \left(n_k L \rho_{sys}^{(n-e_k,m)} + m_k \rho_{sys}^{(n,m-e_k)} L^\dagger \right) \\
& + \left[\rho_{sys}^{(n+e_k,m)}, L^\dagger \right] + \left[L, \rho_{sys}^{(n,m+e_k)} \right] \Bigg),
\end{aligned}
\tag{9}
$$

where bold symbols indicate the vector character of a variable and e_k denotes the unit vector in direction k. The complex coefficients G_i, w_i can be obtained from an exponential fit of the bath correlation function $\alpha(\tau) \approx \sum_i G_i e^{-w_i \tau}$ or inferred from scattering theory [59]. The number of coefficients required for the fit sets the dimension of the vector indices and therefore increases the computational complexity.

This equation has been successfully applied to a wide range of systems [55, 60–65], but a major limitation is the requirement for the entire system density matrix. The latter scales exponentially with the size of the subsystem and is therefore practically inaccessible for the vast majority of many-body quantum systems. Application to many-body systems requires therefore to identify a path that retains the dimensionality of the systems descriptor, thus far $\rho_{sys}^{(n,m)}$, on a manageable level.

An intuitive way to accomplish this is presented by the BBGKY hierarchy which is build around the reduced density matrices (RDM)

$$
\begin{aligned}
F_{123}^{(m,n)} &= N(N-1)(N-2)\, \mathrm{Tr}_{4,5,\dots,N}(\rho^{(m,n)}), \\
F_{12}^{(m,n)} &= N(N-1)\, \mathrm{Tr}_{3,4,\dots,N}(\rho^{(m,n)}), \\
F_{1}^{(m,n)} &= N\, \mathrm{Tr}_{2,3,\dots,N}(\rho^{(m,n)}).
\end{aligned}
\tag{10}
$$

Here $\mathrm{Tr}_{i,i+1,\dots,N}$ denotes the trace over all particles with index larger than i and the reduced density matrices are normalized to the provide the particle number under contraction [66]. Note that since we are restricting ourselves to permutationally symmetric systems the order of indexing is irrelevant.

Our goal in the following is to derive a closed hierarchy of equations for the reduced density matrix F_{12}, such that the (auxiliary) density matrices in Eq. (9) only scale with the square of the dimension of the single-particle Hilbertspace. From Eq. (9) it follows that (see App. B)

$$
\begin{aligned}
\dot{F}_{12}^{(n,m)} =\ & -i[H_1 + H_2, F_{12}^{(n,m)}] + \mathrm{Tr}_3\left([V_{13} + V_{23}, F_{123}^{(n,m)}]\right) - (w \cdot n + w^* \cdot m) F_{12}^{(n,m)} \\
& + \sum_{k=1}^{M} \Bigg(G_k \left(n_k (L_1 + L_2) F_{12}^{(n-e_k,m)} + n_k \mathrm{Tr}_3(L_3 F_{123}^{(n,m)}) + m_k F_{12}^{(n,m-e_k)}(L_1^\dagger + L_2^\dagger) + m_k \mathrm{Tr}_3(L_3^\dagger F_{123}^{(n,m)}) \right) \\
& + \left[F_{12}^{(n+e_k,m)}, L_1^\dagger + L_2^\dagger \right] + \left[L_1 + L_2, F_{12}^{(n,m+e_k)} \right] \Bigg).
\end{aligned}
\tag{11}
$$

For any interacting many-body system, the two-body RDM F_{12} will couple to the three-body RDM F_{123}, which in turn will couple to the four-body RDM and so on. In order to close this hierarchy we therefore need to express the three-body RDM in terms of the one- and two-body RDM

$$
F_{123} \approx \widetilde{F}_{123}(F_{12}, F_1).
$$

We demonstrate in App. B how this can be achieved by reformulating the hierarchy of equations for the density matrices $\rho_{sys}^{(n,m)}$ as an equation for a *single* operator in an extended Hilbertspace $\mathcal{H}_{ext} = \mathcal{H}_{sys} \otimes \mathcal{H}_{aux}$ and subsequently neglecting three-body correlations within the system. However, we keep correlations between two particles in the system and the auxiliary degree of freedom that captures the influence of the environment. With these approximations we arrive at the expression below for the three-body RDM, where we have left out indices

(**0**, **0**) for brevity

$$
\begin{aligned}
\widetilde{F}_{123}^{(\bm{m},\bm{n})} =\, & 4\frac{(N-1)(N-2)}{N^3}\,\mathrm{Tr}(F_1^{(\bm{m},\bm{n})})F_1F_2F_3 \\
& + \frac{N-2}{N}\left(F_{12}F_3^{(\bm{m},\bm{n})}+F_2^{(\bm{m},\bm{n})}F_{13}+F_1^{(\bm{m},\bm{n})}F_{23}\right) \\
& + \frac{N-2}{N}\left(F_1F_{23}^{(\bm{m},\bm{n})}+F_{13}^{(\bm{m},\bm{n})}F_2+F_{12}^{(\bm{m},\bm{n})}F_3\right) \\
& - \frac{N-2}{N^2}\,\mathrm{Tr}(F_1^{(\bm{m},\bm{n})})\left(F_{12}F_3+F_{13}F_2+F_1F_{23}\right) \\
& - 2\frac{(N-2)(N-1)}{N^2}\Big(F_1^{(\bm{m},\bm{n})}F_2F_3 \\
& + F_1F_2^{(\bm{m},\bm{n})}F_3+F_1+F_2F_3^{(\bm{m},\bm{n})}\Big).
\end{aligned}
\tag{12}
$$

Inserting the above approximation into Eq. (11) provides the BBGKY-HEOM equation up to three-body correlations – the central tool of this work. As desired, it represents a closed hierarchy for the two-particle RDM that can account for interactions within the system and simultaneously includes the influence of a generic non-Markovian environment.

$\widetilde{F}_{123}^{(\bm{m},\bm{n})}$ is invariant under particle exchange, but does not preserve the (anti-)symmetry of the wavefunctions as required for (fermionic) bosonic particles. As explained in detail in App. B this can be achieved by employing an (anti-) symmetrization operator which projects $\widetilde{F}_{123}^{(\bm{m},\bm{n})}$ onto the (anti-) symmetric subspace of the the Hilbertspace while retaining its norm [50].

III. RESULTS

Every quantum system is a collection of individual particles, may it be a collection of single-photon emitters or the individual electronic and vibrational degrees of freedom that constitute one such emitter. We demonstrate in the following the applicability, strength, and limitation of BBGKY-HEOM for both of these cases. In particular, we focus on two well known paradigmatic models from quantum optics and condensed matter physics: the driven Tavis-Cummings and Fermi-Hubbard model.

A. Driven-dissipative many-emitter systems

A collection of emitters that share a common mode can interact with it collectively, potentially resulting in burst-like correlated emission known as superradiance. Such phenomena are closely linked to the non-classical dynamic of squeezed spin states. Following a series of simplifications for matter, cavity, and light-matter coupling, one obtains the widely used Dicke Hamiltonian [53]

$$
H_{Dicke} = \omega_a \sum_i \sigma_z^i + \omega_c a^\dagger a + g\sum_i \sigma_x^i(a^\dagger + a).
\tag{13}
$$

The Pauli matrices $\sigma_{x,y,z}^i$ represent the SU(2) algebra of an idealized two-level emitter while $a^\dagger(a)$ are the creation (annihilation) operators of the cavity mode. The collection of emitters can be brought out of equilibrium by continuously pumping energy into the system $H_{drive} = 2\Omega\cos\omega_d t \sum_i \sigma_x^i$. A unitary transformation moves us into a frame that rotates with the driving frequency ω_d. As long as the drive is close to resonance, i.e., $\omega_d \gg \Delta_z, \Delta_x, g, \Omega$ with the detunings $\Delta_z = \omega_a - \omega_d$, $\Delta_c = \omega_c - \omega_d$, we can safely discard counter-rotating terms $e^{i(\omega_d+\omega_{a/c})}$ that oscillate too fast to influence the dynamic of the system. We obtain the paradigmatic driven Tavis-Cummings Hamiltonian

$$
\begin{aligned}
H_{DTC} =\, & \Delta_z \sum_i \sigma_z^i + \Omega\sum_i \sigma_x^i + \Delta_c a^\dagger a \\
& + g\sum_i \left(\sigma_+^i a + \sigma_-^i a^\dagger\right).
\end{aligned}
\tag{14}
$$

We will consider the emitters or spins in the following as our system of interest and the cavity as environment dissipating energy into free space at a rate κ. The bath correlation function is readily obtained, for example from the Heisenberg-Langevin equations [51], as

$$
\alpha(\tau) = g^2\langle a^\dagger(\tau)a(0)\rangle = g^2 e^{(-i\Delta_c-\kappa)\tau}.
\tag{15}
$$

For this simple example a fitting procedure is thus not necessary and we can readily use Eq. (11) with $M = 1$ and $G = g^2, W = i\Delta_c + \kappa$. Using the suggested truncation of the many-body BBGKY hierarchy, we then evolve a hierarchy of 2-particle RDMs, here 4×4 matrices, augmented with the HEOM indices $(\bm{m}, \bm{n})$. The computational complexity is therefore *independent* of the number of emitters as all emitters are identical.

Given the necessary computational resources, we could have just as well decided to directly solve the entire system of N-emitter plus lossy cavity using the Lindblad master equation

$$
\dot\rho = -i[H_{DTC}, \rho] + \kappa\left(a\rho a^\dagger - a^\dagger a\rho - \rho a^\dagger a\right).
\tag{16}
$$

This exact solution will be used to estimate the quality of the BBGKY-HEOM and can be obtained in a collective spin picture $S_k = \sum_i \sigma_k^i$, $k \in \{x, y, z, +, -\}$. The 2^N dimensional system Hilbert space can then be restricted to a basis of $N + 1$ permutationally symmetric Dicke states $\{|N/2, m\rangle, m = -N/2, -N/2 + 1, \ldots, N/2\}$ which results in a linear increase of the relevant basis size with N and therefore a quadratic increase of the Liouville space. However, the collective spin-picture fails as soon as individual emitter-emitter interactions need to be included, resulting in an exponentially growing Hilbert space that prohibits exact solutions for systems larger than a handful of emitter. The computational cost for BBGKY-HEOM on the other hand is unaffected by this change and remains system-size independent. Note, that even if there is no direct interaction in this model the spins still interact indirectly via the cavity mode.
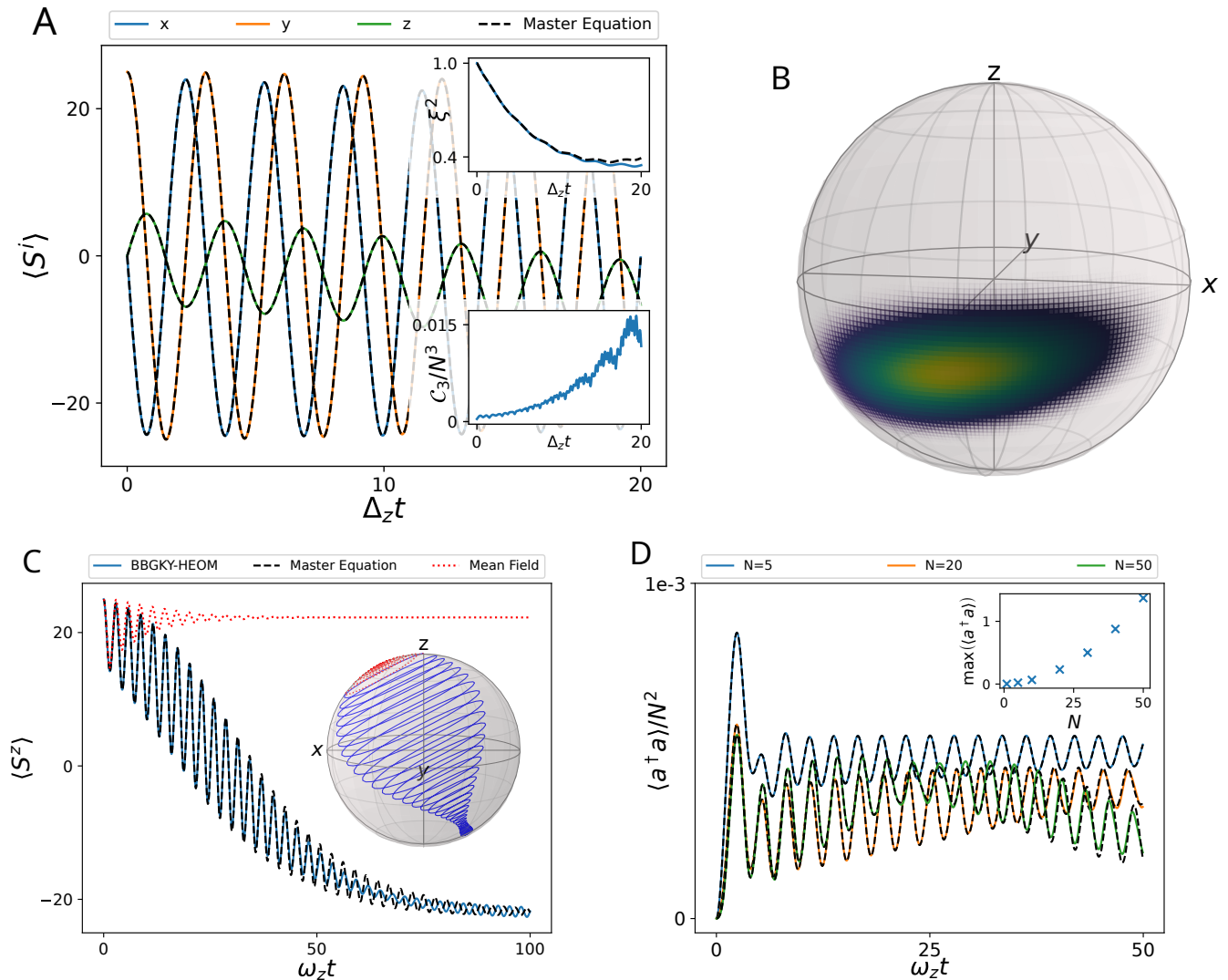
Figure 1: **Squeezing and superradiance in the driven Tavis-Cummings model**: A) Spin dynamic for $N = 50$, $g\sqrt{N}/\kappa = 0.5$, $\Delta_z/\kappa = 0.2$, $\Omega/\kappa = 0.05$, $\Delta_c/\kappa = 10$. B) Corresponding spin-squeezing (see text). C) Superradiant emission from fully excited state. Parameters adjusted to $\Delta_z/\kappa = 2$, $\Delta_x/\kappa = 1$, $\Delta_c/\kappa = 2.4$, $g/\kappa = 0.1$. D) Photon-occupation normalized by N^2 over time and maximum photon number in burst (not normalized) for different N obtained with BBGKY-HEOM. BBGKY-HEOM provides reliable predictions and only begins to deviate slightly at long times when explicit 3-body correlations accumulate to noticeable values.

Fig. 1 (A) illustrates the system dynamic in the rotating frame for $N = 50$ emitter strongly coupled to the cavity $\sqrt{N}g/\kappa = \sqrt{N/4}$ in comparison to the exact solution of the Master equation. The spin components $\langle S_i \rangle$ are accurately predicted within the simulation window, despite the non-classical dynamic of the system. Shown in the upper inset is the spin squeezing (see App. A) which is exhibiting values smaller than unity – a sufficient condition for entanglement. We observes small deviations at long times which can be understood by investigating the slow increase in the explicit 3-body correlations (lower inset), i.e., the term that is discarded in the currently chosen truncation. The spin-squeezing is further illus-

trated by the spin-Q function $Q = \langle \theta, \phi | \rho | \theta, \phi \rangle$ in the upper right subplot (B), with $|\theta, \phi\rangle$ the spin coherent state. Mean-field theory will fail in predicting any of the spin-squeezing effects.

Let us fully excite all emitters and illustrate the resulting superradiant emission in Fig. 1 (C) (parameters adjusted, see caption). BBGKY-HEOM follows closely the exact dynamic and small deviations are visible only close to the fully de-excited steady-state. While mean-field theory models the initial frequency quite accurately, it fails to model the spontaneous emission process and remains trapped at the upper fix-point. The inset projects this dynamic on the Bloch-sphere which illustrates that
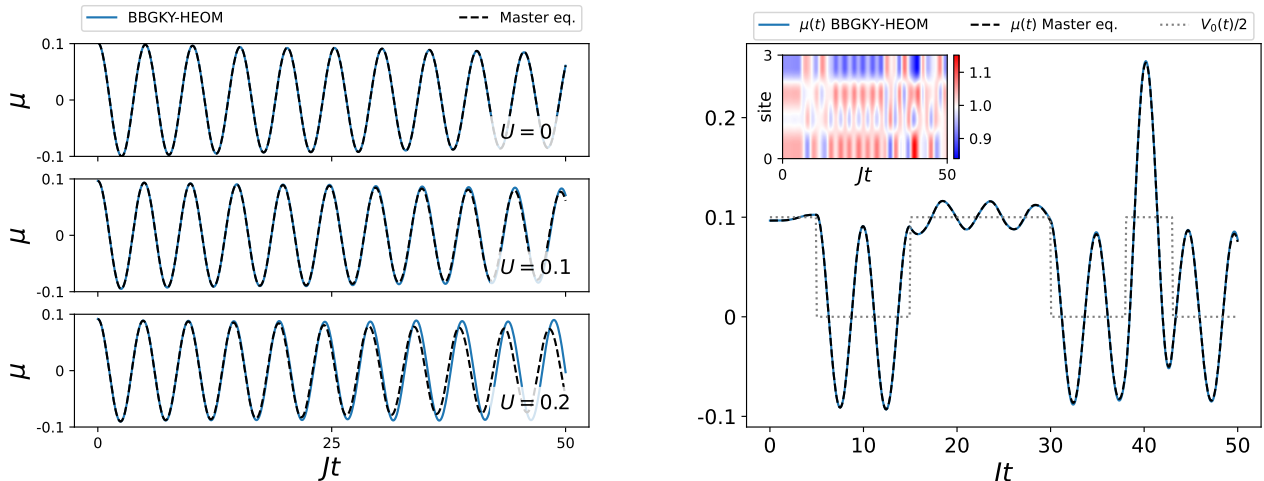
Figure 2: **Fermi-Hubbard model coupled to lossy cavity mode**: (Left) Dynamic of dipole moment of Fermi-Hubbard model ($J = 1$, parameters in text) after site-dependent quench $V(t) = \sum_{i=0}^{3} V_i(t) c_i^\dagger c_i$ with $V_i(0^+) = \frac{1}{5(i+1)}$, which mimics a charge localization event, for different onsite repulsion U. BBGKY-HEOM (blue solid) provides reliable predictions for weak to moderate onsite repulsion when compared to the exact solution (black dashed). (Right) Dipole moment driven by time-dependent potential $V_i(t) = \frac{f(t)}{5(i+1)}$, where f(t) is a step function as shown by the grey dashed line and $U = 0.1$. The example simulates charge noise due to the movement of electrons in the vicinity of the molecule. Inset illustrates onsite occupation.

the failure of the mean field can be connected to restriction to the surface of the sphere while the correct dynamic requires to transverse it diagonally. The sudden increase in the photon number originating from the burst-like emission of N correlated emitter is presented in Fig. 1 (D), demonstrating again accurate predictions by BBGKY-HEOM. Continuous driving results in a continuous replenishment of the cavity mode. The maximum photon-number (inset) is correctly described in its quadratic increase with the emitter number N. In conclusion, BBGKY-HEOM provides accurate predictions for matter and cavity observables at constant cost, i.e., for arbitrary many emitter and with the option to account for direct interaction. We will now relax the simplification of the emitter and instead combine the dynamic of the many-body correlated system with a structured system-bath coupling.

B. Many-body electronic systems coupled to non-Markovian optical environments

The electronic structure of most organic molecules is dominated by covalent bonds or conjugated π-systems, requiring many-body methods to faithfully model their electronic properties. An excitation in such a system cannot be represented by the excitation events of a single electron. Instead, the surrounding electronic cloud reacts and screens the polarization induced by the external field – every optical excitation in a molecule or solid is inherently a many-body process. Electronic correla-

tion can increase to bizarre levels for systems including transition metals, which contribute strongly localized d and f-orbitals shielded from molecular orbitals. Moving two electrons to such a state costs a considerable amount of energy, as they strongly repel each other, resulting in electronic motion that is strongly correlated. A prototypical approach to describe such a system is given by the Hubbard model

$$\hat{H}_H = -J \sum_\sigma \sum_{i=1}^{N} \hat{c}_{i,\sigma}^\dagger \hat{c}_{i+1,\sigma} + \hat{c}_{i+1,\sigma}^\dagger \hat{c}_{i,\sigma} + U \sum_{i=1}^{N} \hat{c}_{i,+\frac{1}{2}}^\dagger \hat{c}_{i,-\frac{1}{2}}^\dagger \hat{c}_{i,-\frac{1}{2}} \hat{c}_{i,+\frac{1}{2}},$$

(17)

with the hopping rate J between two localized Wannier orbitals and the onsite energy U. Usually $U > 0$ as it costs energy to force two electrons on the same site. Weak onsite interaction $U/J \ll 1$ will only marginally limit the free hopping of electrons between the states while extreme values of $U/J \gg 1$ will result in states similar to Wigner crystals [67]. We focus here on small to moderate onsite interactions $U/J < 1$ to account for the weak to moderate correlation in molecular systems.

Naturally, the electronic structure is embedded in an environment of optical (or vibro-phononic) modes, resulting in the emergence of polaritonic states if coupled sufficiently strong. Our BBGKY-HEOM approach allows to consistently describe and monitor how the dynamic of the lossy cavity mode imprints correlations in the electronic many-body system and vice versa. The corresponding

minimal Hamiltonian for such a Cavity-Fermi-Hubbard system [68, 69]

$$\hat{H} = \hat{H}_H + \hbar\omega(\hat{a}^\dagger\hat{a} + \frac{1}{2})$$
$$- \sqrt{\frac{\hbar\omega}{2\varepsilon_0 V}}(\hat{a} + \hat{a}^\dagger)\mathbf{e}_{cav} \cdot \hat{\boldsymbol{\mu}} + \frac{1}{2\varepsilon_0 V}(\mathbf{e}_{cav} \cdot \hat{\boldsymbol{\mu}})^2, \quad (18)$$

includes self-polarization contributions of the localized dipole moment $\hat{\boldsymbol{\mu}} = \mathbf{e}_{chain}\sum_\sigma\sum_{i=1}^N r_i\hat{c}_{i,\sigma}^\dagger\hat{c}_{i,\sigma}$. The local positions $r_i \in \{-\frac{N-1}{2}\Delta, ..., 0, ..., +\frac{N-1}{2}\Delta\}$ as well as their spacing Δ are defined with respect to the center of the PZW gauge [42, 43]. We will use $J = 1$, $\omega = 0.5$, assign a cavity loss of $\kappa = 0.2$, a coupling strength of $g = \sqrt{\frac{\hbar\omega}{2\varepsilon_0 V}} = 0.1$, and disregard the self-polarization for the moment.

One strength of explicitly treating the many-body electronic system is that the electronic response to external stimuli, such as charge noise, can be explicitly modelled. Assume a short polyacetylene molecule with 4 sites hosting 4 electrons, represented by Eq. (18), and initially in equilibrium. A distortion in the surrounding structure suddenly traps an electron near our molecule, resulting in a repulsive Coulomb potential $V(t) = \sum_{i=0}^3 V_i(t)c_i^\dagger c_i$ and $V_i(0^+) = \frac{1}{5(i+1)}$. The subsequently induced dipole moment is presented in Fig. 2 (left) for three different values of onsite repulsion U. Without direct electronic interaction, the BBGKY-HEOM is nearly exact as the many-body correlation induced by the cavity is comparably small in this case. The quality of our approximation remains excellent for $U = 0.1$ and slowly worsens for systems with sizeable correlation of $U = 0.2$, as one would expect.

Charge will not only localize once but randomly tunnel in and out of the impurity. The dynamic originating from the random localization of charge on the dipole moment is shown in Fig. 2 (right) with the corresponding changes in occupation (inset) and time-dependent (gray dotted) potential. Clearly, hitting a resonance condition such as at $Jt = 40$ can result in large deviations from the equilibrium state without noticeable influence on the quality of the BBGKY-HEOM predictions. One strength of the BBGKY-HEOM is therefore to resolve the many-body electronic dynamic that originates from time-dependent modulations which allows us to simulate e.g. charge noise, dynamic screening, or triplet-triplet annihilation explicitly – a feature that we plan to leverage further in the future.

Let us end this section by illustrating the limitations of the BBGKY hierarchy. The 4 sites of our Hubbard-chain host again 4 electrons but we force them initially to occupy the 1st and 3rd site only, i.e., our initial state has two doubly occupied and two empty sites. Naturally, this state is far from the correlated ground-state and results in a violent dynamic of density sloshing forward and backward. Fig. 3 illustrates the onsite occupation, i.e., the electronic density, of the initially occupied sites over time. The exact reference calculations (black dashed)
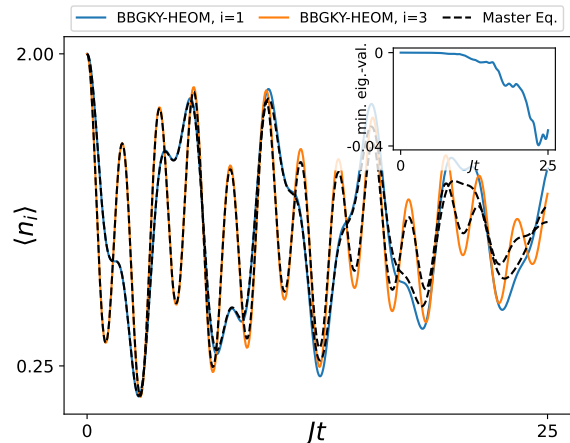

Figure 3: **Strong dynamic in Cavity-Fermi-Hubbard model**: Occupation for second and last site, both initially doubly occupied, over time. Sites 0 and 2 are initially empty, resulting in rapid charge-oscillations between the sites and a quick build-up of 3-body correlations. The BBGKY-HEOM becomes increasingly worse with ongoing time which is accompanied with the appearance of negative eigenvalues in the 1RDM that could potentially lead to instabilities.

follow our predictions closely up to $Jt \approx 20$ before the quality of the BBGKY-HEOM prediction deteriorates. We can relate this sudden loss of accuracy to the appearance of artificial negative eigenvalues in the reduced density matrix (see inset) – a failure caused by the fact that the BBGKY hierarchy is not contraction consistent by default. Contraction consistency refers to the fact that the 2RDM must be obtained from the trace of the approximated 3RDM. Neglecting this condition results in a build-up of negative eigenvalues that will inevitably lead to numerical instabilities. Fortunately, such effects can be circumvented by enforcing contraction consistency via more complex reconstruction functionals $\widetilde{F}_{123}$ as shown in [50, 70]. BBGKY-HEOM is remarkably stable when compared to the bare dynamic of the electronic system alone. We attribute this observation to the fact that the decoherence imprinted by the structured bath penalizes instabilities as large uncontrolled oscillations couple efficiently to the optical mode which dissipates a notable fraction of the energy and thus stabilized the dynamic of the system.

C. Many-body dynamic embedded into organic crystals

Many-body electronic systems, such as molecules or (an)organic frameworks, are often embedded in a liquid or crystalline environment. For example, organic
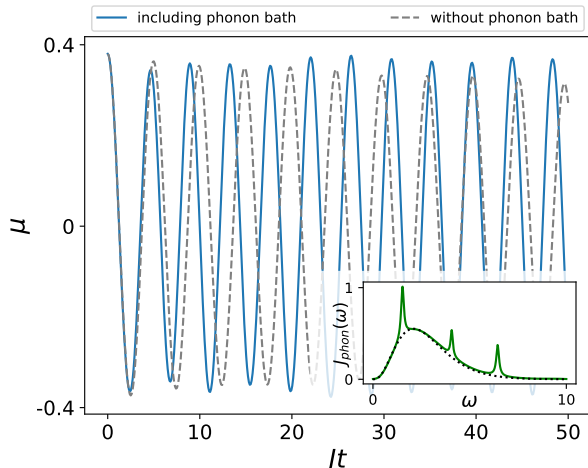
Figure 4: **Cavity-Fermi-Hubbard model under the influence of a complex phonon bath**: The evolution of the electronic dipole with (blue, solid) and without (gray, dashed) the phonon bath after a quench $V_i(0^+) = \frac{4}{5(i+1)}$ induced by charge noise. Parameters are identical to Fermi Hubbard example in previous section with U=0.1. The inset shows the phonon spectral density with $\int J_{phon}(\omega)\mathrm{d}\omega = 0.1^2$ (coupling identical to cavity mode) where the superohmic background is highlighted as black dotted line.

molecules embedded in organic crystals can serve as highly coherent emitter[1], quantum memory[71], or organic light-emitting diode. Their environment is a combination of local vibrational, extended phononic, and photonic modes, giving rise to a highly structured and complex spectral function. BBGKY-HEOM provides now the means to retain the complexity of the electronic structure and combine it with the full system-bath dynamic, i.e., extending beyond previous approaches that relied on a simplified description of the electronic system[72].

Fig. 4 demonstrates the impact of the non-Markovian phonon-bath on the dynamic of the dipole moment of the same 4-site Cavity-Fermi-Hubbard model ($U = 0.1$) subsequent to a quench induced by a charge fluctuation $V_i(0^+) = \frac{4}{5(i+1)}$. As the nuclei move closer together (further apart) their effective hopping rate increases (decreases), which we model by coupling the phonon-bath to the hopping operator:

$$L^{phon} = \sum_{\sigma} \sum_{i=1}^{N} \hat{c}_{i,\sigma}^{\dagger} \hat{c}_{i+1,\sigma} + \hat{c}_{i+1,\sigma}^{\dagger} \hat{c}_{i,\sigma}. \qquad (19)$$

The corresponding phonon spectral density $J_{phon}(\omega)$ is illustrated in the inset, comprising a superohmic background that provides a simplified model for the linear dispersion of the acoustic phonon branch of the crystal as well as additional discrete modes. Neglecting the phonon bath (gray dashed) leads to a strong misrepresentation, which is much larger than the possible deviations caused

by the BBGKY approximation (recall Fig. 2), and clearly shows why a holistic approach to the many-body dynamics of the system and the system-bath interaction is crucial for a predictive description.

IV. CONCLUSION

No quantum system is perfectly isolated and the description of its environment can be essential for our physical understanding. Confined optical or plasmonic modes and vibrational or phononic modes might even challenge the dynamic of a subsystem of interest by strongly coupling to the internal degrees of freedom. Energy deposited in the environment will then not simply decohere but act back on the system, resulting in non-Markovian, or memory dependent, system-bath interaction. The dynamic of the system has often been simplified to the degree that the many-body character inherited by every molecule or solid-state impurity has been lost.

In this study, we presented a rigorous hierarchical approach based on the combination of the reduced density-matrix (BBGKY) and system-bath (HEOM) hierarchy. BBGKY-HEOM is flexible enough to tackle typical quantum optical and condensed matter problems, striking a balance between high accuracy and good performance. In particular, we demonstrated that correlated (superradiant) emission and spin squeezing, i.e., dynamic that extends beyond the capabilities of meanfield theory, is accurately captured. We then leveraged the ability to describe many-body electronic systems, here in the form of the Fermi-Hubbard model, to illustrate the interplay between correlated system dynamic and structured baths by simulating different forms of charge noise. We observed again excellent performance for as long as the onsite repulsion U and the electronic dynamic remain moderate. Finally, we demonstrated the major strength of the BBGKY-HEOM by simulating the interplay between the vibro-phononic bath of an organic crystal coupled to the many-body dynamic of the Cavity-Fermi-Hubbard model. Both contributions, i.e., non-Markovian system-bath coupling and many-body dynamics are equally important – clearly stressing the need for a more holistic perspective on solid-state quantum emitters.

ACKNOWLEDGMENTS

the granting authority can be held responsible for them.

Appendix A: Spin squeezing

The spin squeezing parameter is defined as $\xi^2(t) = N(\Delta S_{\mathbf{n}_1})^2/(\langle S_{\mathbf{n}_2}\rangle^2 + \langle S_{\mathbf{n}_3}\rangle^2)$, where $\mathbf{n}_1(t)\perp\langle\mathbf{S}\rangle(t)$ is obtained, by calculating the vector perpendicular to the current spin direction that has the minimal associated variance $(\Delta S_{\mathbf{n}_1})^2$.

Appendix B: Derivation of the BBGKY-HEOM equations

In the following we detail the derivation of the BBGKY-HEOM equation. For the sake of readability we focus on the case of a scalar index, corresponding to the case where the environment is a damped cavity mode. The extension to a vector index is trivial. Starting from the HEOM equation (9) with the auxiliary density matrix

$$\rho^{(m,p)} = (ig)^m(-ig)^p \operatorname{Tr}_C\left((a^\dagger)^p a^m \rho_{tot}\right), \tag{B1}$$

where ρ_{tot} is the total state of system and cavity mode. We now want to employ the BBGKY hierarchy to reduce the dimension of the system.
We use the same normalization for the reduced density matrices as in the known BBGKY hierarchy,

$$\begin{aligned} F_{123} &= N(N-1)(N-2)\operatorname{Tr}_C(\rho_{123C}), \\ F_{12} &= N(N-1)\operatorname{Tr}_C(\rho_{12C}), \\ F_1 &= N\operatorname{Tr}_C(\rho_{1C}). \end{aligned} \tag{B2}$$

Following Eq. (B1) we define the auxiliary matrices as

$$F_{1..N}^{(m,p)} = (ig)^m(-ig)^p \operatorname{Tr}_C\left((a^\dagger)^p a^m F_{1..N,C}\right). \tag{B3}$$

Their evolution equation can be derived from the HEOM Eq. (9) by tracing over all but N particles and assuming that the density matrix is invariant under particle exchange:

$$\begin{aligned} \dot{F}_{12}^{(m,p)} =& \partial_t N(N-1)(ig)^n(-ig)^m \operatorname{Tr}_{3...N,C}\left((a^\dagger)^m a^n \rho\right), \\ =& N(N-1)\operatorname{Tr}_{3..N}(\dot{\rho}^{(n,m)}), \\ =& -i[H_1 + H_2, F_{12}^{(n,m)}] \\ & - [(n-m)i\Delta + (m+n)\kappa]\,F_{12}^{(n,m)} \\ & + g^2\Big(n(L_1+L_2)F_{12}^{(n-1,m)} + \operatorname{Tr}_3(L_3 F_{123}^{(m-1,p)}) \\ & m\rho^{(n,m-1)}(L_1^\dagger + L_2^\dagger) + \operatorname{Tr}_3(L_3^\dagger F_{123}^{(m,p-1)})\Big) \\ & + \left[F_{12}^{(n+1,m)}, L_1^\dagger + L_2^\dagger\right] + \left[L_1 + L_2, F_{12}^{(n,m+1)}\right]. \end{aligned} \tag{B4}$$

Above we used that

$$\begin{aligned} \operatorname{Tr}_{3...N}([\sum_{i=1}^N H_i, \rho] =& [H_1 + H_2, \rho_{12}] \\ & + \sum_{i=3}^N \operatorname{Tr}_{3...N}(H_i\rho) - \operatorname{Tr}_{3...N}(\rho H_i), \\ =& [H_1 + H_2, \rho_{12}] \\ & + \sum_{i=3}^N \operatorname{Tr}_{3...N}(H_i\rho) - \operatorname{Tr}_{3...N}(H_i\rho), \\ =& [H_1 + H_2, \rho_{12}]. \end{aligned} \tag{B5}$$

In the next step we use a cluster expansion to express the term $F_{123}^{(m,p)}$ in terms of the reduced density one- and two-body matrices. The key approximation that enables this is the neglect of higher order correlations. The cluster expansion amounts to expressing the 3-body density matrix including the cavity as:

$$\begin{aligned} \rho_{123C} =& \rho_1 \otimes \rho_2 \otimes \rho_3 \otimes \rho_C \\ & + \rho_1 \otimes \rho_2 \otimes \Gamma_{3C} + \rho_1 \otimes \Gamma_{23} \otimes \rho_C + \Gamma_{12} \otimes \rho_3 \otimes \rho_C \\ & + \Gamma_{13} \otimes \rho_2 \otimes \rho_C + \Gamma_{1C} \otimes \rho_2 \otimes \rho_3 + \rho_1 \otimes \Gamma_{2C} \otimes \rho_3 \\ & + \Gamma_{12} \otimes \Gamma_{3C} + \Gamma_{1C} \otimes \Gamma_{23} + \Gamma_{13} \otimes \Gamma_{2C} \\ & + \rho_1 \otimes \Gamma_{23C} + \Gamma_{13C} \otimes \rho_2 + \Gamma_{12C} \otimes \rho_3 + \Gamma_{123} \otimes \rho_C \\ & + \Gamma_{1234C} \end{aligned} \tag{B6}$$

We now neglect 3-body correlations within the system $\Gamma_{123} = 0$ as well as four body correlations $\Gamma_{123C} = 0$ to obtain

$$\begin{aligned} \widetilde{F}_{123}^{(m,n)} =& 4\frac{(N-1)(N-2)}{N^3} \operatorname{Tr}(F_1^{(m,n)})F_1 F_2 F_3 \\ & + \frac{N-2}{N}\left(F_{12}F_3^{(m,n)} + F_2^{(m,n)}F_{13} + F_1^{(m,n)}F_{23}\right) \\ & + \frac{N-2}{N}\left(F_1 F_{23}^{(m,n)} + F_{13}^{(m,n)}F_2 + F_{12}^{(m,n)}F_3\right) \\ & - \frac{N-2}{N^2}\operatorname{Tr}(F_1^{(m,n)})\left(F_{12}F_3 + F_{13}F_2 + F_1 F_{23}\right) \\ & - 2\frac{(N-2)(N-1)}{N^2}\Big(F_1^{(m,n)}F_2 F_3 \\ & + F_1 F_2^{(m,n)}F_3 + F_1 + F_2 F_3^{(m,n)}\Big). \end{aligned} \tag{B7}$$

This now leaves us with a reconstruction functional for all auxiliary matrices and enables us to truncate the BBGKY-HEOM equation by neglecting higher order correlations.

Appendix C: Multipolar gauge

Electric and magnetic fields can be expressed in terms of the vector and scalar potentials

$$E = -\nabla\phi - \nabla \cdot A, \qquad (C1)$$

$$B = \nabla \times A, \qquad (C2)$$

where $\dot{A} := \frac{\partial}{\partial t}A$ [73]. The E and B fields are invariant with respect to gauge transformations

$$A' = A - \nabla\chi, \quad \phi' = \phi + \dot{\chi}. \qquad (C3)$$

We define the Green's function for the divergence operator as

$$\nabla \cdot g^{\parallel}(x, x') = -\delta(x - x'). \qquad (C4)$$

We can add to $g^{\parallel}(x, x')$ any transversal vector field $g^{\perp}(x, x')$ and define

$$g_\mu(x, x') = g^{\parallel}(x, x') + \mu g^{\perp}(x, x'). \qquad (C5)$$

The parallel Greens function has the well known representation

$$g^{\parallel}(x, x') = \nabla \frac{1}{4\pi|x - x'|}. \qquad (C6)$$

A possible choice for the perpendicular Green's function is

$$g^{\perp}(x, x') = \int_0^t \mathrm{d}\lambda x' \cdot \delta^{\perp}(\lambda x' - x), \qquad (C7)$$

which corresponds straight line from the origin to the point x'. This particula choice is motivated by the construction of the multipolar gauge [74]. We define a gauge function χ_μ as

$$\chi_\mu(x) = \mu \int \mathrm{d}x' \, g^{\perp}(x', x) A^{\perp}(x'). \qquad (C8)$$

We can thus define new vector potential as

$$A_\mu(x) = A^{\perp}(x) - \mu\nabla\chi(x). \qquad (C9)$$

We can define a polarization field also with the help of the Greens function

$$P_\mu(x) = \int \mathrm{d}x \, g_\mu(x, x')\rho(x'), \qquad (C10)$$

where $\rho(x)$ is the charge distribution. We see immediately that $\nabla \cdot P_\mu(x) = -\rho(x)$. The choice $\mu = 0$ corresponds to a Coulomb gauge and $\mu = 1$ to the multipolar gauge [74]. We may derive the Hamiltonian in arbitrary μ-gauge from a Lagrangian formalism and we find that [43]

$$H = \sum_i \frac{1}{2m_i}(p_i - qA_\mu(r_i))^2 + V$$
$$+ \frac{1}{2}\int \mathrm{d}x \left(\Pi_\mu(x) + P_\mu^{\perp}(x)\right)^2 + (\nabla \times A^{\perp}(x))^2\right), \qquad (C11)$$

where p_i, x_i and $A^{\perp}, \Pi_\mu$ are canonically conjugate and satisfy the commutation relations $[x_{i,a}, p_{j,b}] = i\hbar\delta_{ij}\delta_{ab}$ and $[A_a^{\perp}(x), \Pi_{\mu,b}^{\perp}(x')] = i\hbar\delta_{ab}^{\perp}(x - x')$.

We assume that the center of mass of the system is at the origin and do the electric dipole approximation [43]. The Hamiltonian simplifies to

$$H = \sum_i \frac{(p_i - (1 - \mu)A_\mu(0)^2)^2}{2m} + V \qquad (C12)$$

$$+ \sum_i \mu d_i \cdot \Pi_\mu(0) + \frac{1}{2}\mu^2 \sum_i d_i\delta^{\perp}(0)d_i \qquad (C13)$$

$$+ \frac{1}{2}\int \mathrm{d}x \left(\Pi_\mu(x)^2 + (\nabla \times A^{\perp}(x))^2\right). \qquad (C14)$$

In the Coulomb gauge ($\mu = 0$) we obtain that the coupling to the electromagnetic field is provided by the term $(p_i - A_\mu(0))^2$ leading to the diamagnetic A^2 term.

On the other hand, in the multipolar gauge ($\mu = 1$) the transition dipole of the system d_i couples to the field Π_1. Physically this means that the system couples to the field which is the differnce of the transverse electric field generated bu the transverse vector potential and the polarization field

$$\Pi_1 = E^{\perp} - P^{\perp}. \qquad (C15)$$

In addition a self-polarization term arises.

The choice of the gauge leads to different types of interpretation of the physical nature of the electric field the system couples to. We refer further discussions on this subtle points to literature [43, 73–75]

Appendix D: Derivation of the HEOM

We sketch here a derivation of the HEOM equations. We assume that the system is coupled to the environment via operator q. The response of the system to the environment is given by the bath correlation function $\alpha(t)$. For HEOM we need that the bath correlation function is of the form

$$\alpha(t) = Ge^{-Wt}, \qquad (D1)$$

where G and W may be complex numbers. The reduced dynamics of the system can be written in the path integral form

$$\rho_t(q, q') = \int \mathrm{d}q_0 \int \mathrm{d}q_0' \int \mathcal{D}q \int \mathcal{D}q'$$
$$\times e^{i(S[q] - S[q'])} F[q, q']\rho_0(q_0, q_0), \qquad (D2)$$

where $S[q]$ is the action of the closed system and $\rho_t(q, q') = \langle q| \rho_t |q'\rangle$. The influence functional contains all information about the coupling of the open system to the environment. In this case it reads

$$F[q, q'] = e^{-\int_0^t \mathrm{d}s \int_0^s \mathrm{d}s' \, (q_s - q_s')\left(\alpha(s-s')q_{s'} - \alpha^*(s-s')q_{s'}'\right)}. \qquad (D3)$$

We define auxiliary states

$$\rho_t^{n,m}(q, q') = = \int dq_0 \int dq_0' \int \mathcal{D}q \int \mathcal{D}q'$$
$$\times e^{i(S[q]-S[q'])} F[q,q'] \rho_0(q_0,q_0) Q_t^n Q_t'^m, \tag{D4}$$

where $Q_t = \int_0^t ds\, \alpha(t-s) q_s$ and $Q_t' = \int_0^t ds\, \alpha^*(t-s) q_s'$. Then by directly computing the time derivative of the auxiliary state and by using the exact expression for the open system dynamics together with the special form of the bath correlation function we directly arrive to

$$\dot{\rho}_t^{n,m} = -i[H, \rho_t^{n,m}] - (nW + mW^*)\rho_t^{n,m}$$
$$+ [\rho_t^{n+1,m}, q] + [q, \rho_t^{n,m+1}]$$
$$+ nGq\rho_t^{n+1,m} + mG^*\rho_t^{n,m+1}q. \tag{D5}$$

The equations presented in the main text are a generalization of the above equations in two respects. First, we allow for multiple exponential terms in the expansion for the bath correlation function, and second we allow for the case $q \neq q^\dagger$.

Appendix E: Numerical details

Numerical simulations were performed with the python packages numpy[76], scipy[77] and qutip[78]. The BBGKY-HEOM equation (11) with the approximation for the three-body reduced density matrix given in Eq. (12) were solved with the scipy implementation of the explicit Runge-Kutta method of order 5(4), with an absolute tolerance of $1e-10$ and dynamical timestepping. We checked for the convergence with respect to the hierarchy depth, which justifies a hierarchy depth of 5 for the Tavis-Cummings model and 3 for the Cavity-Fermi-Hubbard model. The benchmark simulations for the quantum master equation were performed using qutips mesolve function with default parameters.

[1] C. Toninelli, I. Gerhardt, A. Clark, A. Reserbat-Plantey, S. Götzinger, Z. Ristanović, M. Colautti, P. Lombardi, K. Major, I. Deperasińska, *et al.*, Single organic molecules for photonic quantum technologies, Nature Materials **20**, 1615 (2021).

[2] N. P. de Leon, K. M. Itoh, D. Kim, K. K. Mehta, T. E. Northup, H. Paik, B. S. Palmer, N. Samarth, S. Sangtawesin, and D. W. Steuerman, Materials challenges and opportunities for quantum computing hardware, Science **372**, eabb2823 (2021), https://www.science.org/doi/pdf/10.1126/science.abb2823.

[3] J. M. Gambetta, J. M. Chow, and M. Steffen, Building logical qubits in a superconducting quantum computing system, npj Quantum Information **3**, 10.1038/s41534-016-0004-0 (2017).

[4] M. Fleischhauer and M. D. Lukin, Quantum memory for photons: Dark-state polaritons, Physical Review A **65**, 022314 (2002).

[5] D. M. Coles, N. Somaschi, P. Michetti, C. Clark, P. G. Lagoudakis, P. G. Savvidis, and D. G. Lidzey, Polariton-mediated energy transfer between organic dyes in a strongly coupled optical microcavity, Nature Materials **13**, 712 (2014).

[6] J. Feist and F. J. Garcia-Vidal, Extraordinary exciton conductance induced by strong coupling, Phys. Rev. Lett. **114**, 196402 (2015).

[7] C. Schäfer, M. Ruggenthaler, H. Appel, and A. Rubio, Modification of excitation and charge transfer in cavity quantum-electrodynamical chemistry, Proceedings of the National Academy of Sciences **116**, 4883 (2019).

[8] G. Jarc, S. Y. Mathengattil, A. Montanaro, F. Giusti, E. M. Rigoni, R. Sergo, F. Fassioli, S. Winnerl, S. Dal Zilio, D. Mihailovic, *et al.*, Cavity-mediated thermal control of metal-to-insulator transition in 1t-tas2, Nature **622**, 487 (2023).

[9] C. Schäfer and D. G. Baranov, Chiral polaritonics: analytical solutions, intuition, and use, The Journal of Physical Chemistry Letters **14**, 3777 (2023).

[10] F. J. Garcia-Vidal, C. Ciuti, and T. W. Ebbesen, Manipulating matter by strong coupling to vacuum fields, Science **373**, eabd0336 (2021), https://www.science.org/doi/pdf/10.1126/science.abd0336.

[11] T. S. Haugland, C. Schäfer, E. Ronca, A. Rubio, and H. Koch, Intermolecular interactions in optical cavities: An ab initio qed study, The Journal of Chemical Physics **154**, 094113 (2021).

[12] S. Latini, D. Shin, S. A. Sato, C. Schäfer, U. D. Giovannini, H. Hübener, and A. Rubio, The ferroelectric photo ground state of srtio¡sub¿3¡/sub¿: Cavity materials engineering, Proceedings of the National Academy of Sciences **118**, e2105618118 (2021), https://www.pnas.org/doi/pdf/10.1073/pnas.2105618118.

[13] T. Leppälä, A. G. Abdelmagid, H. A. Qureshi, K. S. Daskalakis, and K. Luoma, Linear optical properties of organic microcavity polaritons with non-markovian quantum state diffusion, Nanophotonics (2024).

[14] A. G. Abdelmagid, H. A. Qureshi, M. A. Papachatzakis, O. Siltanen, M. Kumar, A. Ashokan, S. Salman, K. Luoma, and K. S. Daskalakis, Identifying the origin of delayed electroluminescence in a polariton organic light-emitting diode, Nanophotonics (2024).

[15] C. Schäfer, J. Flick, E. Ronca, P. Narang, and A. Rubio, Shining light on the microscopic resonant mechanism responsible for cavity-mediated chemical reactivity, Nature Communications **13**, 7817 (2022).

[16] W. Ahn, J. F. Triana, F. Recabal, F. Herrera, and B. S. Simpkins, Modification of ground-state chemical reactivity via light–matter coherence in infrared cavities, Science **380**, 1165 (2023), https://www.science.org/doi/pdf/10.1126/science.ade7147.

[17] M. Piejko, B. Patrahau, K. Joseph, C. Muller, E. Devaux, T. W. Ebbesen, and J. Moran, Solvent polarity under vibrational strong coupling, Journal of the American Chemical Society **145**, 13215 (2023), pMID: 37289656, https://doi.org/10.1021/jacs.3c02260.

[18] M. Castagnola, T. S. Haugland, E. Ronca, H. Koch, and C. Schäfer, Collective strong coupling modifies aggregation and solvation, The Journal of Physical Chemistry Letters **15**, 1428 (2024), pMID: 38290530, https://doi.org/10.1021/acs.jpclett.3c03506.

[19] A. Mandal, M. A. Taylor, B. M. Weight, E. R. Koessler, X. Li, and P. Huo, Theoretical advances in polariton chemistry and molecular cavity quantum electrodynamics, Chemical Reviews **123**, 9786 (2023).

[20] C. Schäfer, J. Fojt, E. Lindgren, and P. Erhart, Machine learning for polaritonic chemistry: Accessing chemical kinetics, Journal of the American Chemical Society **146**, 5402–5413 (2024).

[21] D. Sidler, T. Schnappinger, A. Obzhirov, M. Ruggenthaler, M. Kowalewski, and A. Rubio, Unraveling a cavity induced molecular polarization mechanism from collective vibrational strong coupling (2024), arXiv:2306.06004 [quant-ph].

[22] L. P. Lindoy, A. Mandal, and D. R. Reichman, Quantum dynamical effects of vibrational strong coupling in chemical reactivity, Nature Communications **14**, 2733 (2023).

[23] O. Siltanen, K. Luoma, and K. S. Daskalakis, Incoherent polariton dynamics and nonlinearities in organic light-emitting diodes, arXiv preprint arXiv:2404.04257 (2024).

[24] C.-Y. Chan, M. Tanaka, Y.-T. Lee, Y.-W. Wong, H. Nakanotani, T. Hatakeyama, and C. Adachi, Stable pure-blue hyperfluorescence organic light-emitting diodes with high-efficiency and narrow emission, Nature Photonics **15**, 203 (2021).

[25] V. Link, K. Luoma, and W. T. Strunz, Non-markovian quantum state diffusion for spin environments, New Journal of Physics **25**, 093006 (2023).

[26] N. Megier, W. T. Strunz, C. Viviescas, and K. Luoma, Parametrization and optimization of gaussian non-markovian unravelings for open quantum dynamics, Physical review letters **120**, 150402 (2018).

[27] W. T. Strunz, L. Diósi, and N. Gisin, Open system dynamics with non-markovian quantum trajectories, Phys. Rev. Lett. **82**, 1801 (1999).

[28] Y. Tanimura, Nonperturbative expansion method for a quantum system coupled to a harmonic-oscillator bath, Phys. Rev. A **41**, 6676 (1990).

[29] Y. Tanimura, Stochastic liouville, langevin, fokker–planck, and master equation approaches to quantum dissipative systems, Journal of the Physical Society of Japan **75**, 082001 (2006), https://doi.org/10.1143/JPSJ.75.082001.

[30] L. Chen, Y. Zhao, and Y. Tanimura, Dynamics of a one-dimensional holstein polaron with the hierarchical equations of motion approach, The Journal of Physical Chemistry Letters **6**, 3110 (2015), pMID: 26267210, https://doi.org/10.1021/acs.jpclett.5b01368.

[31] J. Bätge, Y. Ke, C. Kaspar, and M. Thoss, Nonequilibrium open quantum systems with multiple bosonic and fermionic environments: A hierarchical equations of motion approach, Phys. Rev. B **103**, 235413 (2021).

[32] H. Liu, L. Zhu, S. Bai, and Q. Shi, Reduced quantum dynamics with arbitrary bath spectral densities: Hierarchical equations of motion based on several different bath decomposition schemes, The Journal of Chemical Physics **140**, 134106 (2014), https://pubs.aip.org/aip/jcp/article-pdf/doi/10.1063/1.4870035/15476905/134106_1_online.pdf.

[33] Y. Yang, R. Chikkaraddy, Q. Lin, D. D. A. Clarke, D. Wigger, J. J. Baumberg, and O. Hess, Electrochemically switchable multimode strong coupling in plasmonic nanocavities, Nano Letters **24**, 238 (2024), pMID: 38164905, https://doi.org/10.1021/acs.nanolett.3c03814.

[34] H. Carmichael, *Statistical Methods in Quantum Optics 1: Master Equations and Fokker-Planck Equations*, Physics and astronomy online library (Springer, 1999).

[35] P. Fowler-Wright, B. W. Lovett, and J. Keeling, Efficient many-body non-markovian dynamics of organic polaritons, Phys. Rev. Lett. **129**, 173001 (2022).

[36] M. Mootz, M. Kira, and S. W. Koch, Sequential build-up of quantum-optical correlations, J. Opt. Soc. Am. B **29**, A17 (2012).

[37] N. M. Hoffmann, C. Schäfer, N. Säkkinen, A. Rubio, H. Appel, and A. Kelly, Benchmarking semi-classical and perturbative methods for real-time simulations of cavity-bound emission and interference, The Journal of Chemical Physics **151**, 244113 (2019), https://pubs.aip.org/aip/jcp/article-pdf/doi/10.1063/1.5128076/15568734/244113_1_online.pdf.

[38] V. Link, K. Müller, R. G. Lena, K. Luoma, F. m. c. Damanet, W. T. Strunz, and A. J. Daley, Non-markovian quantum dynamics in strongly coupled multimode cavities conditioned on continuous measurement, PRX Quantum **3**, 020348 (2022).

[39] C. J. S. Martínez, J. Feist, and F. J. García-Vidal, A mixed perturbative-nonperturbative treatment for strong light-matter interactions (2024), arXiv:2312.15324 [quant-ph].

[40] A. Frisk Kockum, A. Miranowicz, S. De Liberato, S. Savasta, and F. Nori, Ultrastrong coupling between light and matter, Nature Reviews Physics **1**, 19 (2019).

[41] F. Beaudoin, J. M. Gambetta, and A. Blais, Dissipation and ultrastrong coupling in circuit qed, Physical Review A **84**, 043832 (2011).

[42] C. Schäfer, M. Ruggenthaler, V. Rokaj, and A. Rubio, Relevance of the quadratic diamagnetic and self-polarization terms in cavity quantum electrodynamics, ACS Photonics **7**, 975 (2020).

[43] A. Stokes and A. Nazir, Implications of gauge freedom for nonrelativistic quantum electrodynamics, Rev. Mod. Phys. **94**, 045003 (2022).

[44] V. Link, H.-H. Tu, and W. T. Strunz, Open quantum system dynamics from infinite tensor network contraction (2024), arXiv:2307.01802 [quant-ph].

[45] S. Flannigan, F. Damanet, and A. Daley, Many-body quantum state diffusion for non-markovian dynamics in strongly interacting systems, Physical Review Letters **128**, 10.1103/physrevlett.128.063601 (2022).

[46] A. J. Daley, Quantum trajectories and open many-body quantum systems, Advances in Physics **63**, 77–149 (2014).

[47] N. Schlünzen, J.-P. Joost, and M. Bonitz, Achieving the scaling limit for nonequilibrium green functions simulations, Phys. Rev. Lett. **124**, 076601 (2020).

[48] R. Tuovinen, Y. Pavlyukh, E. Perfetto, and G. Stefanucci, Time-linear quantum transport simulations with correlated nonequilibrium green's functions, Phys. Rev. Lett. **130**, 246301 (2023).

[49] A. Akbari, M. J. Hashemi, A. Rubio, R. M. Niem-
inen, and R. van Leeuwen, Challenges in truncating
the hierarchy of time-dependent reduced density ma-
trices equations, Physical Review B **85**, 10.1103/phys-
revb.85.235121 (2012).

[50] S. Donsa, F. Lackner, J. Burgdörfer, M. Bonitz, B. Kloss,
A. Rubio, and I. Březinová, Nonequilibrium correlation
dynamics in the one-dimensional fermi-hubbard model:
A testbed for the two-particle reduced density matrix
theory, Phys. Rev. Res. **5**, 033022 (2023).

[51] H.-P. Breuer and F. Petruccione, *The Theory of Open
Quantum Systems* (Cambridge University Press, 2007).

[52] A. Miglio, V. Brousseau-Couture, E. Godbout, G. Anto-
nius, Y.-H. Chan, S. G. Louie, M. Côté, M. Giantomassi,
and X. Gonze, Predominance of non-adiabatic effects in
zero-point renormalization of the electronic band gap,
npj Computational Materials **6**, 167 (2020).

[53] C. C. Gerry and P. L. Knight, *Introductory Quantum
Optics* (Cambridge University Press, 2005).

[54] N. Makri, The linear response approximation and its low-
est order corrections: An influence functional approach,
The Journal of Physical Chemistry B **103**, 2823 (1999).

[55] Y. Tanimura, Numerically "exact" approach to open
quantum dynamics: The hierarchical equations of
motion (HEOM), The Journal of Chemical Physics **153**,
020901 (2020), https://pubs.aip.org/aip/jcp/article-
pdf/doi/10.1063/5.0011599/15575870/020901_1_online.pdf.

[56] C.-Y. Hsieh and J. Cao, A unified stochastic formulation
of dissipative quantum dynamics. I. Generalized hierar-
chical equations, The Journal of Chemical Physics **148**,
014103 (2018), https://pubs.aip.org/aip/jcp/article-
pdf/doi/10.1063/1.5018725/13764391/014103_1_online.pdf.

[57] C.-Y. Hsieh and J. Cao, A unified stochas-
tic formulation of dissipative quantum dynam-
ics. II. Beyond linear response of spin baths,
The Journal of Chemical Physics **148**, 014104
(2018), https://pubs.aip.org/aip/jcp/article-
pdf/doi/10.1063/1.5018726/13764525/014104_1_online.pdf.

[58] U. Weiss, *Quantum Dissipative Systems (Third Edition)*,
Series In Modern Condensed Matter Physics (World Sci-
entific Publishing Company, 2008).

[59] D. Lentrodt and J. Evers, Ab initio few-mode theory for
quantum potential scattering problems, Phys. Rev. X **10**,
011008 (2020).

[60] T. P. Fay and D. T. Limmer, Coupled charge and energy
transfer dynamics in light harvesting complexes from
a hybrid hierarchical equations of motion approach, J.
Chem. Phys. **157**, 10.1063/5.0117659 (2022).

[61] J. Ma, Z. Sun, X. Wang, and F. Nori, Entanglement dy-
namics of two qubits in a common bath, Phys. Rev. A
85, 062323 (2012).

[62] A. Kato and Y. Tanimura, Quantum heat current
under non-perturbative and non-markovian conditions:
Applications to heat machines, J. Chem. Phys. **145**,
10.1063/1.4971370 (2016).

[63] J. Jin, X. Zheng, and Y. Yan, Exact dynamics of dissi-
pative electronic systems and quantum transport: Hier-
archical equations of motion approach, J. Chem. Phys.
128, 10.1063/1.2938087 (2008).

[64] A. Ishizaki and G. R. Fleming, Unified treatment of quan-
tum coherent and incoherent hopping dynamics in elec-
tronic energy transfer: Reduced hierarchy equation ap-
proach, J. Chem. Phys. **130**, 10.1063/1.3155372 (2009).

[65] R. Härtle, G. Cohen, D. R. Reichman, and A. J. Mil-
lis, Decoherence and lead-induced interdot coupling in
nonequilibrium electron transport through interacting
quantum dots: A hierarchical quantum master equation
approach, Phys. Rev. B **88**, 235426 (2013).

[66] M. Bonitz, *Quantum Kinetic Theory* (Springer Interna-
tional Publishing, Cham, Switzerland, 2016).

[67] D. P. Arovas, E. Berg, S. A. Kivelson, and S. Raghu,
The hubbard model, Annual review of condensed matter
physics **13**, 239 (2022).

[68] J. Li, D. Golez, G. Mazza, A. J. Millis, A. Georges, and
M. Eckstein, Electromagnetic coupling in tight-binding
models for strongly correlated light and matter, Phys.
Rev. B **101**, 205140 (2020).

[69] U. Mordovina, C. Bungey, H. Appel, P. J. Knowles,
A. Rubio, and F. R. Manby, Polaritonic coupled-cluster
theory, Phys. Rev. Res. **2**, 023262 (2020).

[70] F. Lackner, I. Březinová, T. Sato, K. L. Ishikawa, and
J. Burgdörfer, Propagating two-particle reduced den-
sity matrices without wave functions, Phys. Rev. A **91**,
023412 (2015).

[71] S. L. Bayliss, D. W. Laorenza, P. J. Mintun, B. D.
Kovos, D. E. Freedman, and D. D. Awschalom,
Optically addressable molecular spins for quantum
information processing, Science **370**, 1309 (2020),
https://www.science.org/doi/pdf/10.1126/science.abb9352.

[72] C. Clear, R. C. Schofield, K. D. Major, J. Iles-Smith,
A. S. Clark, and D. P. S. McCutcheon, Phonon-induced
optical dephasing in single organic molecules, Phys. Rev.
Lett. **124**, 153602 (2020).

[73] D. Craig and T. Thirunamachandran, *Molecular Quan-
tum Electrodynamics: An Introduction to Radiation-
molecule Interactions*, Dover Books on Chemistry Series
(Dover Publications, 1998).

[74] R. Woolley, *Foundations of Molecular Quantum Electro-
dynamics* (Cambridge University Press, 2022).

[75] C. Cohen-Tannoudji, J. Dupont-Roc, and G. Grynberg,
*Photons and Atoms: Introduction to Quantum Electro-
dynamics* (Wiley, 1989).

[76] C. R. Harris, K. J. Millman, S. J. van der Walt, R. Gom-
mers, P. Virtanen, D. Cournapeau, E. Wieser, J. Tay-
lor, S. Berg, N. J. Smith, R. Kern, M. Picus, S. Hoyer,
M. H. van Kerkwijk, M. Brett, A. Haldane, J. F. del Río,
M. Wiebe, P. Peterson, P. Gérard-Marchant, K. Shep-
pard, T. Reddy, W. Weckesser, H. Abbasi, C. Gohlke,
and T. E. Oliphant, Array programming with NumPy,
Nature **585**, 357 (2020).

[77] P. Virtanen, R. Gommers, T. E. Oliphant, M. Haber-
land, T. Reddy, D. Cournapeau, E. Burovski, P. Pe-
terson, W. Weckesser, J. Bright, S. J. van der Walt,
M. Brett, J. Wilson, K. J. Millman, N. Mayorov, A. R. J.
Nelson, E. Jones, R. Kern, E. Larson, C. J. Carey, İ. Po-
lat, Y. Feng, E. W. Moore, J. VanderPlas, D. Laxalde,
J. Perktold, R. Cimrman, I. Henriksen, E. A. Quintero,
C. R. Harris, A. M. Archibald, A. H. Ribeiro, F. Pe-
dregosa, P. van Mulbregt, and SciPy 1.0 Contributors,
SciPy 1.0: Fundamental Algorithms for Scientific Com-
puting in Python, Nature Methods **17**, 261 (2020).

[78] J. R. Johansson, P. D. Nation, and F. Nori, QuTiP 2:
A Python framework for the dynamics of open quantum
systems, Comput. Phys. Commun. **184**, 1234 (2013).